



Effect of the Shape of Reinforcement around Openings on Concrete Beams Subjected To Cyclic Loads

Ali Fawzy*

Civil Engineering Department, Faculty of Engineering, Al-Azhar University, Cairo, Egypt

*Corresponding author

Arafa EL-Helloty

Civil Engineering Department, Faculty of Engineering, Al-Azhar University, Cairo, Egypt

M. Hassan Mahmoud

Civil Engineering Department, Faculty of Engineering, Al-Azhar University, Cairo, Egypt

Abstract

Openings in reinforced concrete beams, which were before a structural problem, are now necessary for contemporary construction. These openings enable the seamless integration of HVAC, electrical, and plumbing systems, enhancing functionality, efficiency, and adaptability, and reducing the disruption of future upgrades. Careful engineering guarantees structural integrity, which benefits both building users and constructors through these astute design decisions. This study examines the impact of shear reinforcement and transverse opening height under cyclic loads. This study uses an experimental setup and finite element analysis (ANSYS 19.2) to examine how a reinforced concrete beam with an opening behaves. Specifically, we subjected the middle third of the beam's length to cyclic loads, specifically compression. The test had six beams, unlike the control beam (without opening), and the two main variables were the height of the opening and the special reinforcement around it provided by stirrups. We divided into two groups. The first group included three beams with openings at varying heights and without diagonal reinforcement around the openings. Three beams with openings made up the second group, which also featured diagonal reinforcement around the openings. The opening sizes used in this study were 300*100*60 mm, 300*100*100 mm, and 300*100*120 mm. All the beam specimens have a cross-section of 300*100 mm and a total length of 2000 mm. We tested the beams at two points until they failed. We have discussed the response by examining the deformation in all beams, the pattern of cracks, the modes of failure, and the load-deflection curves that result from cyclic loading at the opening, in the middle span, and on the opposite side of the opening. Results indicated that the load failure of the beams without diagonal reinforcement decreased by a rate ranging from 85% to 90% of the value of the load failure of the beams with diagonal reinforcement surrounding the openings. The results also showed that the load failure rate goes down as the opening height goes up, which corresponds to opening heights of 20%, 30%, and 40% of the beam's height.

Keywords

Reinforced Concrete beams, Web Opening, Cyclic loads, Experimental, Finite elemnt analysis, Diagonal reinforcement, Shear failure, Rectangular opening

1. Introduction

Reinforced concrete is the material of choice for constructing most structures, primarily because of its numerous advantages [1-5]. Consequently, the study of concrete has been progressively growing throughout the years [6-10]. Much work has been done on reinforced concrete beam openings in recent years. Beams generally have openings drilled into them to provide conduits for civil plants like air conditioning, power, and computer networks, We observed that the opening locations varied between the shear zone and the flexural zone as shown in figure 1 [11]. Prior research has examined how concrete beams with and without openings, as well as those with openings and reinforcing surrounding them, behave when subjected to static loads, in addition to strengthening the openings formed during casting using fiber and metal panels. Examining the cyclic loads on reinforced concrete beams with openings, as well as the geometry of the reinforcement surrounding the openings, is crucial.



Fig. 1 Web openings in RC beams [11]

Shallow (Ordinary) Beams

This study examines shallow beams, a specific category of reinforced concrete beams with openings. Certain design regulations, such as the ACI 318M-11 Code [11] and the Egyptian Code (2020) [2], consider a beam to be shallow when:

- | | |
|--|--|
| 1- ACI 318M-11 Code [12] | 2- Egyptian code (2020) [13] |
| $L_n \setminus h > 4$ or $a \setminus h > 2$ | $L \setminus d > 4$ or $a \setminus d > 2$ |

The effective span of the beam is indicated by (L), while the clear span is indicated by (L_n). The shear span is represented by (a), and the height of the beam is indicated by (h).

When the overall cross-sectional area of a beam is decreased, its simple beam behavior transitions into one that is more complex. Multiple research investigations have been conducted on reinforced concrete beams that feature web openings. A load that is repeatedly applied to a material or structure is called a cyclic load. This type of loading can be utilized on a substance or structure to simulate the effects of environmental conditions or extended usage. Wind, waves, and earthquakes are instances of cyclic loads caused by natural factors. Subjecting the structure or material to different loading levels allows one to analyze the effects of repeated loads. In a similar manner, Darwin, 1984 [14] examined light-reinforced concrete cyclic behavior. Their study focused on cantilever beams of lightly reinforced concrete, where they examined cyclic behavior in relation to reinforcement ratio, stirrup capacity, spacing, and a negative to positive reinforcement ratio. Their findings revealed a correlation between maximum shear stress reduction, concrete strength, and nominal stirrup capacity, resulting in improved performance under cyclic load. Likewise, Amiri, 2004 [15] Investigated the impact of circular openings on ultimate strength, flexural strength, and shear strength. They examined the concrete's strength, opening position, and reinforcement placement around the opening. They accomplished this for both regular and high-strength concrete, using a reference beam devoid of any openings. They inspected symmetrical, concentrated loads. Their findings revealed that at large opening diameters, the ultimate strength decreased, and the cracking pattern changed as a mode of failure. Similarly, Amiri, 2011 [16] an investigation was conducted to analyze the effects of openings on the behavior of concrete beams without additional reinforcement in the opening zone using the Finite Element Method (FEM). The results of this study indicate that the ultimate load capacity of RC rectangular section beams is not affected by the performance of beams with circular openings that have a diameter smaller than 0.48 times the depth of the beam web (D). However, if a circular opening with a diameter greater than 0.48 D is included, the ultimate load capacity of the RC rectangular section beams is reduced by at least 26%. Likewise, Latha, 2017 [17] studied the behavior of reinforced concrete beams with openings. The program ANSYS 10.0, which uses the finite element method, has been applied to simulate the behavior of simply supported reinforced concrete beams. These beams include circular openings of different sizes, and the simulation is conducted in three dimensions using a nonlinear finite element method. Rectangular beams made of reinforced concrete that have circular openings with a diameter less than 44% of the beam's depth (D) do not affect the ultimate load capacity. However, if the diameter of the circular openings exceeds 44% of D , it reduces the ultimate load capacity by at least 34.29%. Likewise, Kamonna, 2020 [18] The study entails conducting an experimental investigation into the use of near-surface mounted steel bars to provide support to a deep beam constructed with reinforced concrete and including openings. Thirteen reinforced concrete deep beams with simple support are currently undergoing testing using a two-point load as part of an experimental activity. As a result of the tests, specimens with square openings near the loading points, square openings along the load path, and rectangular openings had final loads that were 49%, 56%, and 70% lower than those without these openings in the beam. Bai, 2013 [19] this study looks into how FRP-confined concrete with a high rupture strain reacts to cyclic axial compression and how to model it. It is the first study to do so. The combined impact of loading cycles and the compressive stress-strain curve of the envelope is initially analyzed by presenting experimental findings. Evidence shows that a cyclic stress-strain model can reliably predict the test results. The suggested cyclic stress-strain model is created by combining an existing cycle stress-strain model, which predicts the unloading and reloading pathways, with an existing monotonic stress-strain model, which predicts the envelope curve. This cyclic stress-strain model can simulate the response of large rupture-strain FRP-jacketed RC columns to seismic loads. Similarly, Biao Li, 2017 [20] an empirical study was conducted to examine the stress-strain

characteristics of steel fiber-reinforced concrete under uniaxial cyclic compression. An increase in the volume fraction of steel fiber can result in a significant reduction in the buildup of plastic strain and an increase in the ratio of elastic stiffness. However, the fiber aspect ratio has the same impact. Medic, 2018 [21] Conducted an empirical investigation on the behavior of reinforced concrete beams under cyclic loading. Specific results from the studies indicated that a restricted zone at the bottom of the beam concentrated major cracks. The length of the zone is equivalent to the height of the beam's cross-section. The hysteresis damping was calculated for specific loading phases. The SAP 2000 program was used to simulate beams with various constitutive laws for concrete and reinforcement, as well as variable cross-section definitions. Similarly, Rita Giao, 2019 [22] achieved a parametric study of reinforced concrete beams critical zones under cyclic loads to evaluate the gravity load on them by a non-linear numerical model. The numerical findings are evaluated based on the overall hysteresis response, total energy dissipation, and equivalent viscous damping ratio. This numerical investigation revealed that the applied load trajectory influences the hysteresis behavior. Likewise, Liu, 2020 [23] This research looks at what happens to the flexural performance of reinforced concrete (RC) beams in metro stations when there are multiple transverse web openings, both when the loads are static and when they are cycling. Five beams, each with a varying number of web openings, are manufactured and subjected to static and cyclic loads. This enables simulation of real-world operations in unfavorable situations. The findings indicate that the presence of the openings reduces the load-carrying capacity, flexibility, rigidity, and ability to dissipate energy of the reinforced concrete beams. Furthermore, the findings indicate that the corners of the openings are the beams' most vulnerable sections. Additionally, Ribeiro, 2020 [24] Do a full analysis of the numerical and experimental tests of an I-beam made of concrete that is being bent under cyclic loads. The Concrete Damaged Plasticity Model (CDP) was utilized in the Abaqus finite element program to simulate the cyclic bending test. The experimental data were used to evaluate various constitutive models for concrete. The results confirm the well-constructed numerical model's efficacy in accurately simulating the cyclic loading bending test. Furthermore, the suggested global damage estimates illustrate the consistency between computational and experimental models. Similarly, Chiu, 2024 [25] The study examined the reinforcement techniques employed in a reinforced concrete beam with a circular opening in the plastic hinge area, which is subject to cyclic loading. Most of the stirrups around the beam opening, without any additional reinforcement, developed yield conditions and were unable to bear the lateral force at a drift ratio of 4%. Crack propagation around the reinforced opening was smaller than that observed throughout the entire specimen. Several previous studies have examined the strengthening of openings by utilizing Carbon fiber-reinforced polymer and steel plates in the presence of loads. Among these investigations: Ahmed, 2012 [26] Examines reinforced concrete beams that have gaps in their web. Analyzing and designing reinforced concrete (RC) beams that have transverse web openings. Additionally, it is advisable to enhance the strength of the reinforced concrete (RC) beams by using externally bonded Fiber Reinforced Polymer (FRP) materials and steel plates. In another study, Rania salih, 2020 [27] Researchers have investigated a Reinforced Concrete Beam with Openings Strengthened Using Fiber-Reinforced Polymer Sheets under Cyclic Load. The addition of fiber-reinforced polymer sheets significantly improves the cyclic behavior of reinforced concrete beams, resulting in an increase in maximum strength and ultimate displacement to approximately 66.67% and 77.14%, respectively. On the other hand, Agag, 2020 [28] Performed an experimental evaluation of several methods for strengthening reinforced concrete beams with openings. Different techniques were utilized to strengthen the area around the opening, either by using externally bonded sheets of carbon fiber-reinforced polymers (CFRP) or by reinforcing the interior with diagonal or additional steel bars placed at the top and bottom positions before the casting process. The addition of internal reinforcements to the beam resulted in a greater ultimate load compared to the beam without any openings. Similarly, Alansary, 2022 [29] studied the behavior an analysis of the shear behavior of reinforced concrete beams with a web opening near the supports. The improvement in the structural performance of these beams resulting from the reinforcement of the openings with external carbon fiber-reinforced polymer (CFRP) sheets was evaluated. The experimental findings indicated that the inclusion of sizable openings decreased the shear strength of reinforced concrete beams by as much as 35% when compared to a solid beam. Furthermore, compared to beams of the same design without CFRP, reinforcing the web opening with CFRP sheets resulted in a 21% and 28% enhancement in shear capacity. Additionally, Khalf, 2023 [30] this study investigates the numerical modeling of reinforced concrete (RC) beams using the ANSYS-standard finite element analysis software. It also proposes reinforcement methods in case it becomes necessary to drill rectangular or circular openings within the beam's shear zones under different applied service load levels. Carbon atoms primarily compose carbon fibers. The strengthened reinforced polymer opening significantly improved the overall structural behavior of the beams. Irrespective of the initial shape, the service load reaches around 40% of the maximum design strength and does not impact the bearing capacities of the reinforced opening RC beams. From the previous literature, it was evident that some studies examined the effects of cyclic loads on both compression and tension, specifically focusing on cyclic loads under compression. These studies also examined beams with or without openings and beam openings with or without additional reinforcement. Therefore, we initiated this study to examine cyclic loads in a single direction (i.e., compression), while maintaining a constant beam opening location and length. We adjusted the opening height as a percentage of the beam height with or without diagonal reinforcement. This is due to insufficient research linking the opening height with different shape reinforcement around opening under cyclic loads to concrete behavior.

2. Experimental Program

2.1 Material Properties

The concrete mix was used to cast all specimens for the experimental work, with a water-cement ratio of 0.50, achieving a cube compressive strength of 35 MPa after 28 days. Regarding the reinforcement steel, the longitudinal steel was high-tensile. Figure 2 shows a steel tensile testing machine. It was used for bottom and top reinforcement, while the transverse reinforcement was normal mild steel, and the stirrups were placed at 150 mm intervals.

2.2 Description of Specimens

The experimental program involved casting seven reinforced concrete beams with a cross-section measuring 100mm×300mm and a total length of 2000mm. Figure 4. Three high-tensile steel bars, each measuring 10 mm in diameter, served as the primary reinforcement at the bottom of each beam, while two other high-tensile steel bars, also measuring 10 mm in diameter, served as the top reinforcement. Additionally, we fitted 6mm stirrups to all beams, spacing them 150mm apart, and placed two longitudinal reinforcements with a diameter of 8mm at both the top and bottom sections of the opening. The top and bottom cords of the opening featured 6mm stirrups, spaced 100 mm apart. Figure 5 illustrates the addition of diagonal reinforcement around beam openings No. (B21, B22, and B23). We installed three linear variable differential transformers (LVDTs) to measure the deformation at three different locations: the mid-span, the opening, and the opposite side of the opening. Table 1 outlines the categorization of the specimens into three groups. Throughout the testing phase, we subjected all beams to two-point loading, as shown in Figure 4. We simultaneously constructed concrete cubes with dimensions of 150x150x150mm and conducted compressive strength tests on the loaded specimens, as illustrated in Figure 3. Control group consists of one beam without opening (the control beam). The group (1) consists of three beams with varying height openings (i.e., 20, 30, and 40% of the beam height), without diagonal reinforcement, and subjected to cyclic load. The group (2) includes three beams with varying height openings (i.e., 20, 30, and 40% of the beam height), with diagonal reinforcement, and subjected to cyclic load.

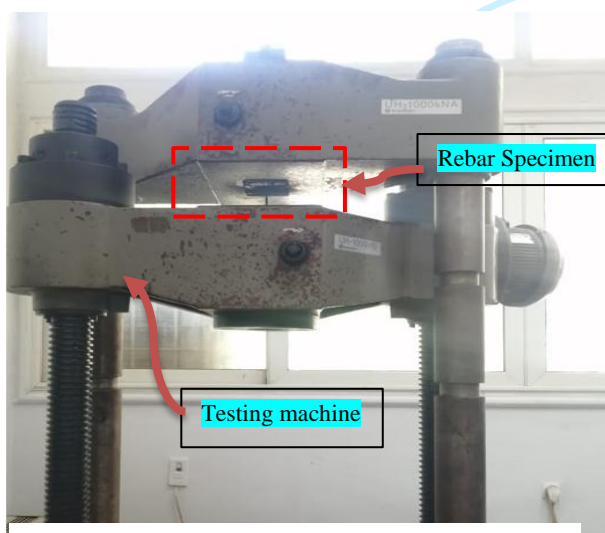


Fig. 2 Steel testing machine

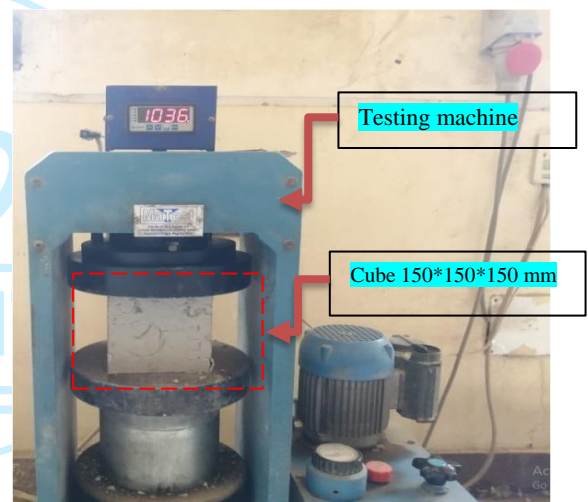


Fig. 3 Cube testing machine

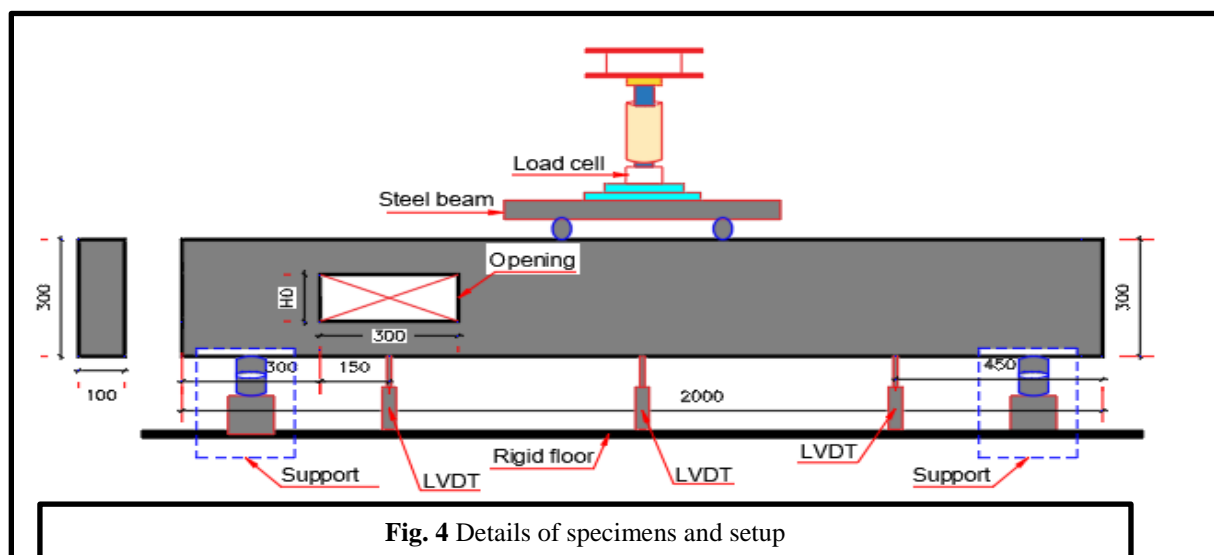


Fig. 4 Details of specimens and setup

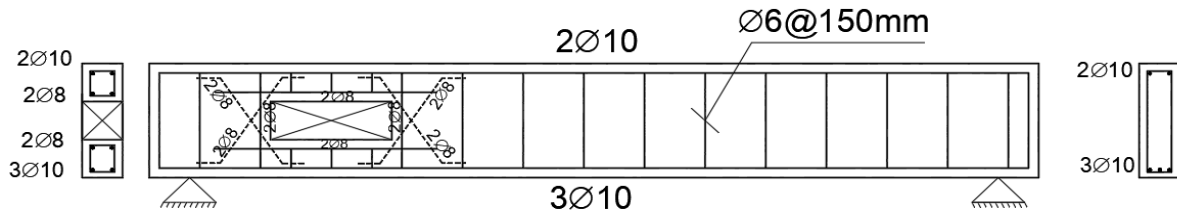


Fig. 5 Details of specimen's with diagonal reinforcement

Table 1 Parameters of specimens

Group No.	Beam No.	Opening Diameter		Depth ratios: (opening/beam)	Concrete strength (f_{cu} N/mm ²)	Bottom Reinforcement	Top Reinforcement	Stirrups	Diagonal reinforcement
		L0 (mm)	H0 (mm)						
Control beam	B0	0	0	0%	35	3Ø10	2Ø10	Ø6 @ 150mm	Without opening
1	B-11	300	60	20%	35	3Ø10	2Ø10	Ø6 @ 150mm	Without diagonal bar
	B-12	300	100	30%	35	3Ø10	2Ø10	Ø6 @ 150mm	Without diagonal bar
	B-13	300	120	40%	35	3Ø10	2Ø10	Ø6 @ 150mm	Without diagonal bar
2	B-21	300	60	20%	35	3Ø10	2Ø10	Ø6 @ 150mm	With diagonal bar
	B-22	300	100	30%	35	3Ø10	2Ø10	Ø6 @ 150mm	With diagonal bar
	B-23	300	120	40%	35	3Ø10	2Ø10	Ø6 @ 150mm	With diagonal bar

3. Nonlinear Finite Element Analysis

This section's goal is to verify the validity of the material models and finite elements by simulating the numerous Dregions taken into consideration in the current work using the ANSYS 19.2 software environment. The validation is completed by comparing the load-deflection curves from the analysis to those from the experimental tests.

3.1 ANSYS Theoretical Background and basic Equations

ANSYS was selected to be employed in this study as it proved its reliability worldwide. The ANSYS FEM code has extensive capabilities, including linear and nonlinear arrays governed by constitutive laws with multiple solvers. The structure's displacement and stress fields are analyzed by ANSYS. Its analytical approach follows nonlinear analysis, which incorporates linear approximation and gradual application of loads per increment. This is executed iteratively until convergence occurs [32]. Theoretically, ANSYS is based on FE, where FE is a numerical approach capable of solving partial-differential equations, which represent the reinforced concrete beams, as elements of a continuous field.

Equation wise, this field is represented by finite nodal quantities, where its formulation is based on the principle of virtual work variation [33], which is characterized by a volume "V" that is bounded by a surface that is represented by the following derivation [32]:

$$\delta U^{(e)} = \delta W^{(e)} \quad (1)$$

Where:

$\delta U^{(e)}$: virtual strain energy

$\delta W^{(e)}$: virtual work of external forces on $\delta U^{(e)}$

$\delta W^{(e)}$: expressed by a matrix notation, as follows:

$$\delta U^{(e)} = \int_V \int \delta \varepsilon^T \sigma dV \quad (2)$$

$$\delta W^{(e)} = \int_S \delta \Psi_s^T T dS \quad (3)$$

Where:

$\delta \varepsilon$: Strains vector induced by vector of virtual displacement " " where:

d : used at virtual displacements

σ : stress vector

T : surface force/area matrix

The displacement function is related to the nodal displacements d by a shape function:

$$\Psi_s = N_s d \quad (4)$$

Where:

N_s : shape function matrix evaluated at the surface S at traction “ T ”

However, strains are linked to nodal displacements:

$$\varepsilon = Bd \tag{5}$$

Stresses are related to strains, as follows

$$\sigma = D\varepsilon \tag{6}$$

Where:

B : strain displacement matrix

D : element material matrix

Substituting equation (4) into (6), the following equation was derived:

$$\delta d^T \left(\int \int_V \int B^T DB dV \right) d = \delta d^T \int \int_S N_s^T T dS \tag{7}$$

Where:

$\int \int_V \int B^T DB dV$: element stiffness matrix K

$\int \int_S N_s^T T dS$: surface loads vector “ f_s ”.

Equation (7) is finite element discretization basic equation, which is rewritten, as follows:

$$Kd = f_s \tag{8}$$

The detailed formulation is presented in [32] However, in order to determine displacement vector “ d ”, by ANSYS [32].

3.2 Material Properties and FE Modeling

Compressive uni-axial stress-strain behavior has an elasto-plastic work hardening model has been used to simulate compressive uni-axial stress-strain behavior, with a perfectly plastic response ending at the point of crashing. Meanwhile, a stress stiffening model has been used to simulate concrete under tension. Up until the first crack, the initial modulus of elasticity is applied. The propagation of cracks is then taken into consideration using a smeared crack model. For steel, linear hardening up to the steel ultimate strength (f_u) was employed after an elastic behavior up to the steel yield stress (f_y). Fig. (6) and Fig. (7) Show the stress-strain curve for concrete and steel reinforcement respectively. SOLID65, a solid element with eight nodes, is used in the FE platform to describe plain concrete. For 3D modeling of solids with or without reinforcing bars (rebar), SOLID65 is utilized. Like concrete, the solid can fracture in tension and be crushed in compression as shown in Fig. (8). the bearing plates are modeled using SOLID 185. A two-node-defined LINK 180 element is utilized to model the steel bars is shown in Fig. (9).

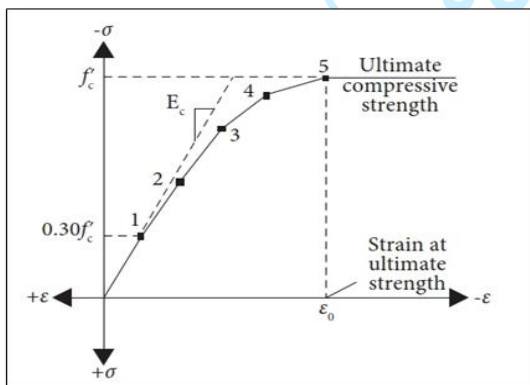


Fig. 6 Simplified compressive uniaxial Curve for concrete [31]

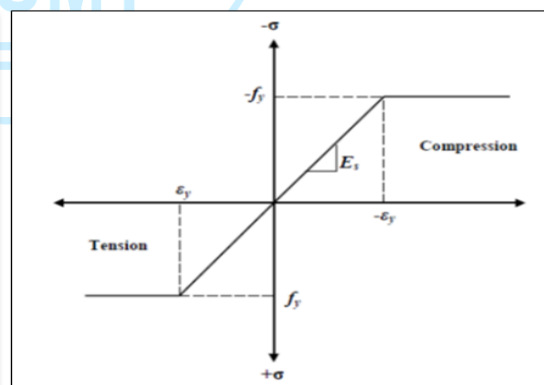


Fig. 7 Stress strain curve for steel Stress-strain reinforcement [13]

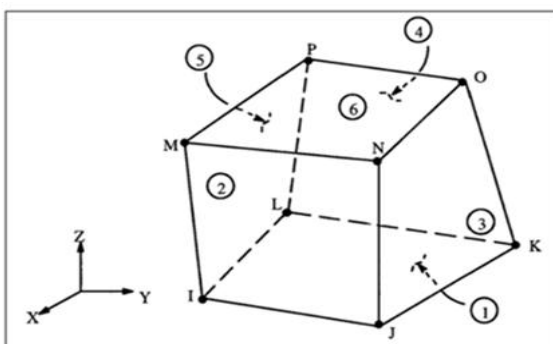


Fig. 8 Concrete SOLID65 [32]

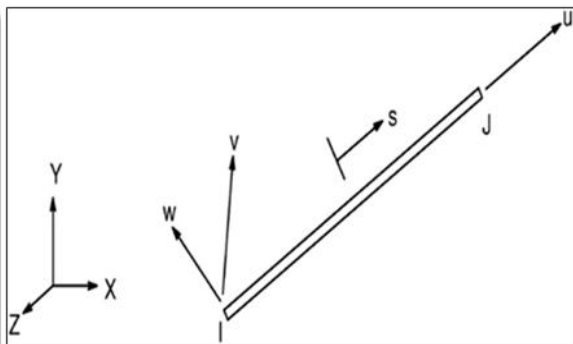


Fig. 9 3-D reinforcement LINK 180 [32]

3.3 Numerical Simulation of the Specimen Loading

The model was run to replicate the specimens under loading after the discretization procedure. On the other hand, Figure 10 illustrates the geometry of the beams, while Figures 11 and 12 show the results. Showcase the diagonal bar and non-diagonal bar reinforcement for the beams, exposing three specimens (without diagonal bar around opening) and three specimens (with diagonal bar around opening) to cyclic load. The cyclic loading protocol was to apply a very small vertical displacement that incrementally increased to 0.50 mm until reaching the point of failure. This systematic approach to loading was selected to represent the progressive beam response to cyclic loading.

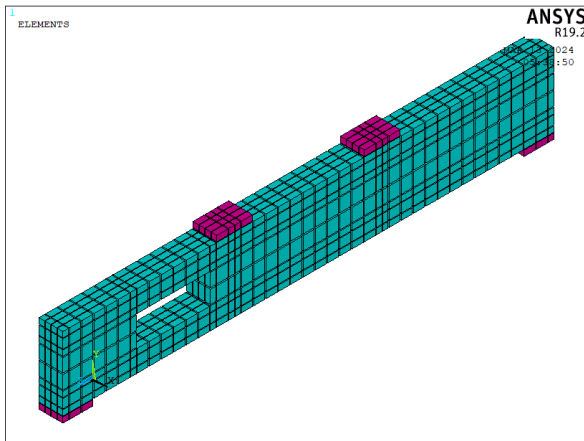


Fig.10 Discretized specimen

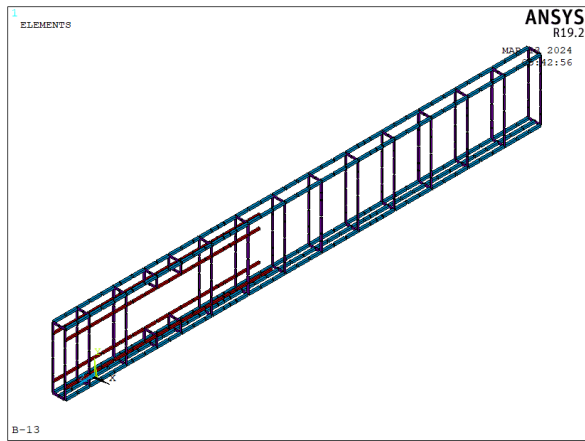


Fig 11 Beam reinforcement without diagonal bar



Fig.12 Beam reinforcement with diagonal bar surrounding openings

4. Results and Discussion

We acquired, investigated, and graphically presented the experimental and finite element results. Table 2 illustrates the failure modes, load failure, and maximum deflection for the tested specimens at the mid-span, opening, and opposite opening. In Figure 13, you can see the failure load estimates for Group 1 (without diagonal reinforcement around openings) and Group 2 (with diagonal reinforcement around openings). These estimates come from both experiments and finite element analyses. When diagonal reinforcement was placed around the opening, the beams' behavior improved.

Table 2 Experimental and FE analyzed results

Beam No.	Load failure (KN)		Deflection (mm) due to static and cyclic loads						Mode failure	Reinforcement surrounding opening
			At mid span		At opening		Opposite to opening			
	Exp.	FEA	Exp.	FEA	Exp.	FEA	Exp.	FEA		
B0	110	115	5.00	4.50	4.20	3.90	4.20	3.90	flexural	Without opening
B11	100	105	7.50	7.80	7.40	7.90	5.80	5.60	Shear at opening	Without diagonal
B12	68	72	7.10	6.80	6.60	6.30	5.40	5.70	Shear at opening	Without diagonal
B13	60	63	6.20	6.0	6.10	6.0	4.80	4.00	Shear at opening	Without diagonal
B21	110	108	11.00	8.00	9.00	7.00	7.00	5.50	Shear at opening	With diagonal
B22	80	77	8.00	7.10	7.80	6.40	5.90	5.00	Shear at opening	With diagonal
B23	70	70	6.30	4.50	5.50	4.00	4.00	3.00	Shear at opening	With diagonal

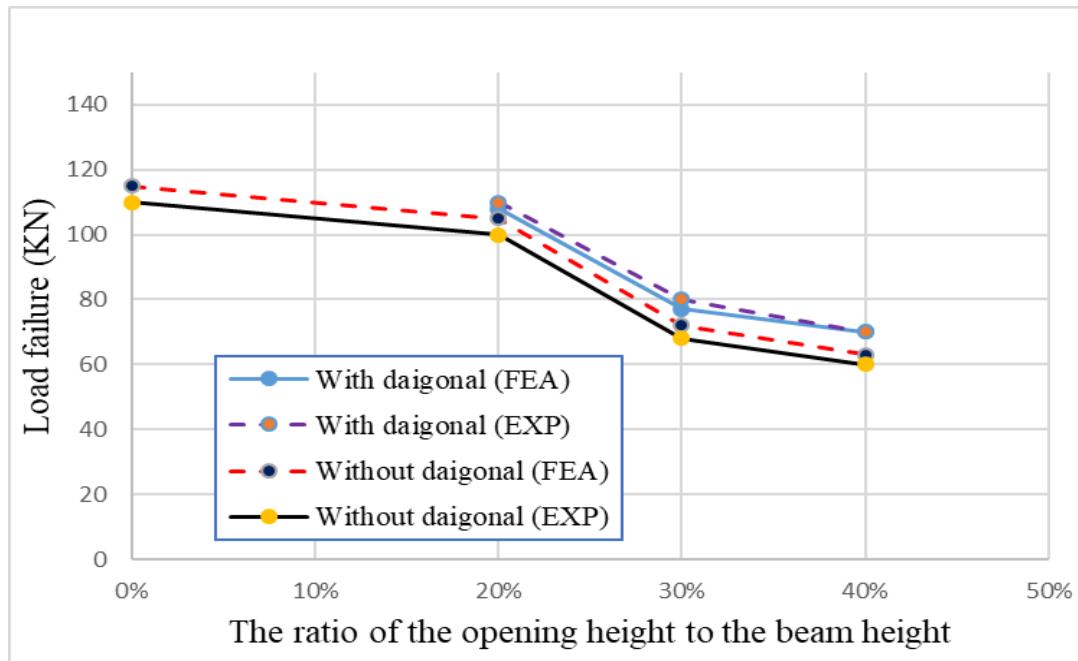


Fig. 13 compares the beams failure load without and with a diagonal.

4.1 Cracks Pattern

Specimens B0

Figure 14 show the cracking history of specimen B0 (without opening), subjected to cyclic loads. The first crack, a flexural crack with a load level of 56 KN, occurred at midspan. Under increased loading, the cracks moved away from the center and spread diagonally towards the supports, thereby passing the characteristics to the beam. Crushing occurred at load levels of 110 KN for experimental, 115 KN for finite element. Cyclic loading leads to fatigue failure in materials, where repeated stress cycles cause progressive damage and ultimately cracking. This is particularly common in materials like concrete.

Specimens B 11 and B 21

First cracks appeared in the corners of the top opening under a load of 31 KN and 37 KN, respectively, when we made an opening in the beam at a height equivalent to 20% of the beams height as shown in figure 15-a and 16-a. With increasing loading, cracks spread in the middle of the beams and near the supports, and the concentration of cracks around the opening increased until the beams reached a failure load of 100 KN and 110 KN in the experiment, and 105 KN and 108 KN for finite element. In the case of an opening with a height equivalent to 20% of the beam height and without diagonal reinforcement around the opening, the failure load decreased by 10% from the load of the control beam. In the case of beams equipped with diagonal reinforcement around the openings, the failure load decreased by 3% of the control beam load.

Specimens B12 and B22

When the height of the opening increased from 20% to 30% of the height of the beam, the initial cracks appeared at a lower load of 21 KN and 26 KN, and the beam collapsed at a load of 68 KN and 80 KN for experimental, and 72 KN and 77 KN for finite elements. The cracks dispersed throughout the beam and centered around the opening, as depicted in Figures 15-b and 15-b. It is worth noting that when the beam is without diagonal reinforcement, the failure load decreases by 11%.

Specimens B13 and B23

Figures 15-c and 16-c show the cracks that occurred on beams with openings at a height equivalent to 40% of the beam's height when subjected to cyclic loads. The first cracks appeared around the opening at loads of 19 KN and 23 KN, respectively, and the cracks began to spread and increase in concentration around the opening until the beam reached the failure at load 60 KN, 70 KN for experimental and 63 KN, 70 KN for finite element. Cracks appeared at the support and the middle of the beam and were concentrated around the openings. It is important to mention that without diagonal reinforcement in the beam, there is a 13% decrease in the failure load.

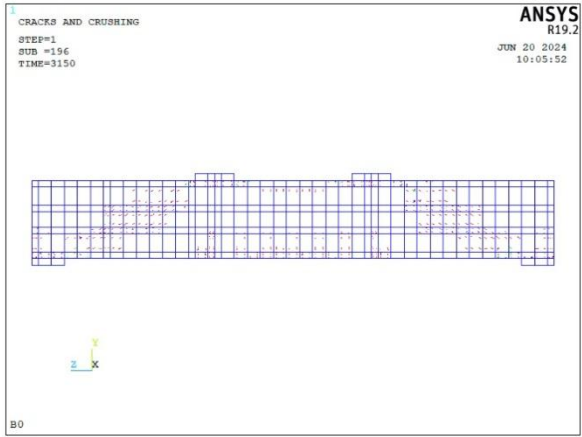
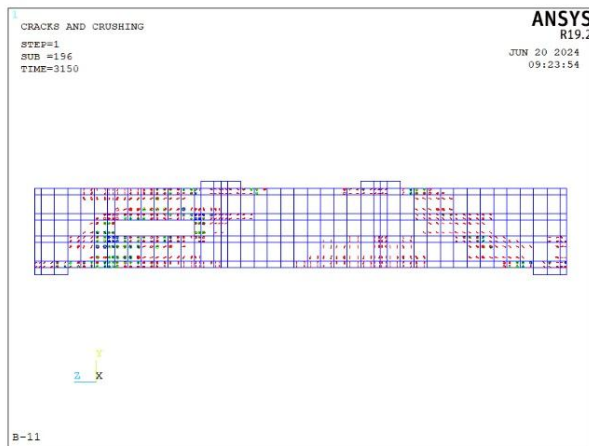
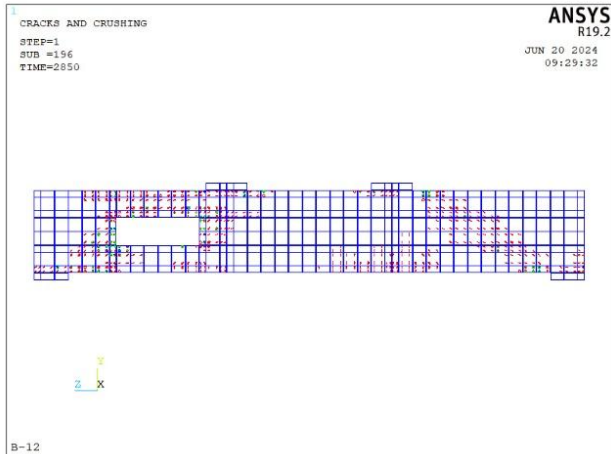


Fig. 14 Experimental and numerical comparison of specimen cracks



(a) B11 specimen



(b) B12 specimen



(c) B13 specimen

Fig.15 Cracks in beams without diagonal reinforcement

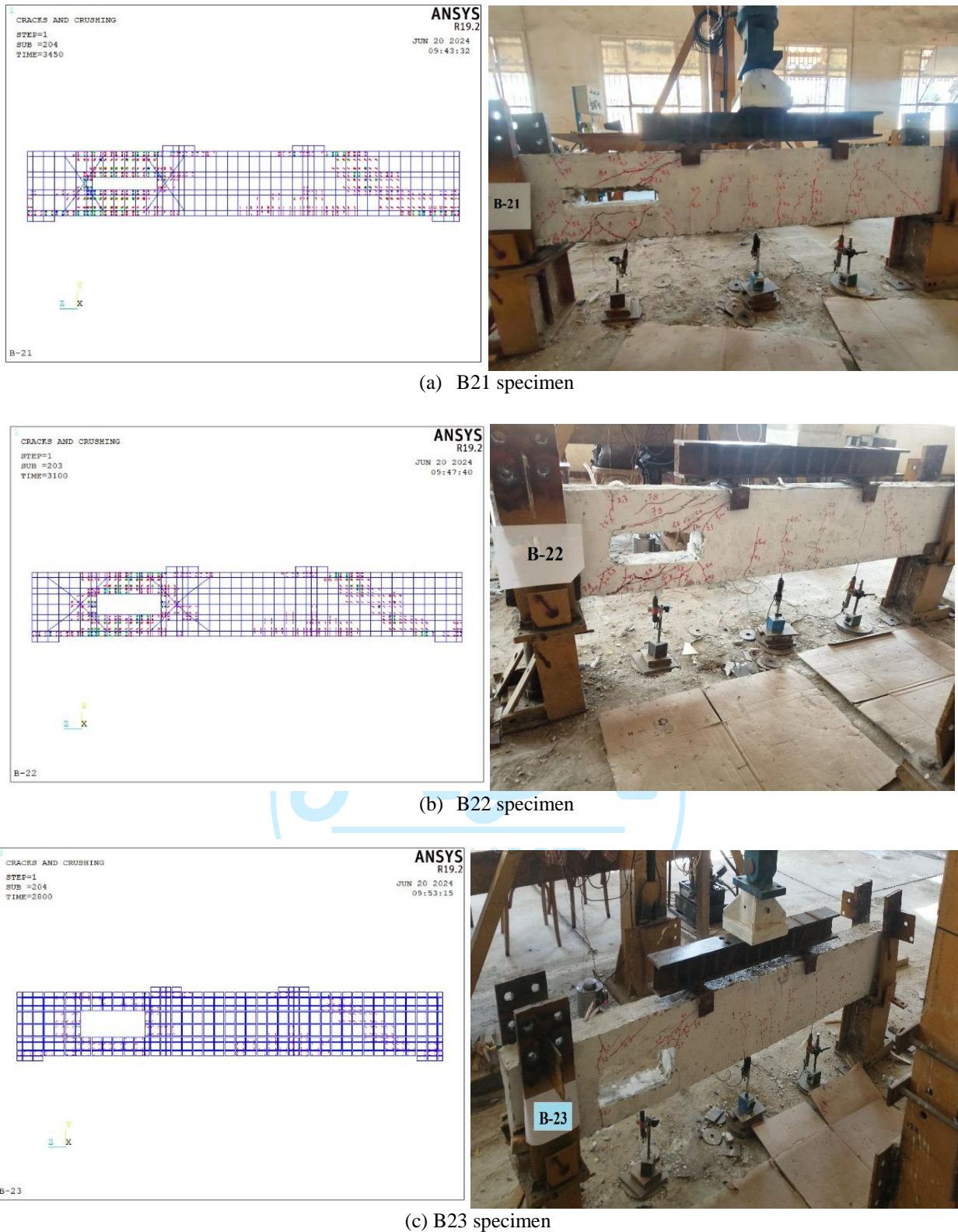


Fig. 16 Cracks in beams with diagonal reinforcement

4.2 Deformation Shape

The control beam (i.e., B0), without openings, experienced the most deformation in the mid-span. As the height of the opening increased, the deformation of beams (i.e., B11, B12, and B13) without diagonal reinforcement around openings approached the shear zone. Beams (i.e., B21, B22, and B23) with diagonal reinforcement surrounding the openings showed an evenly distributed deformation. Figure 17 illustrates this, with the blue tint indicating the maximum deformation caused by the cyclic load in the beam.

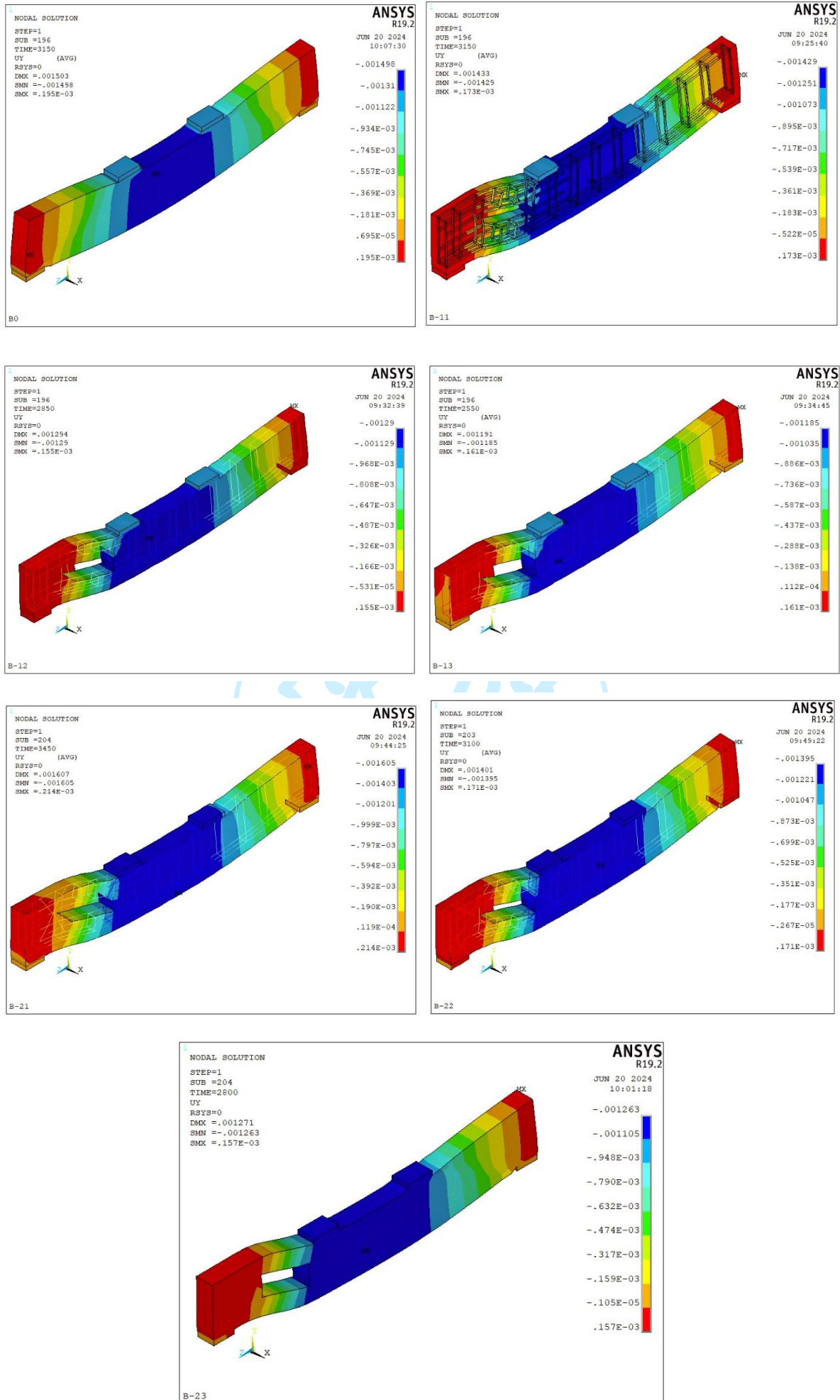
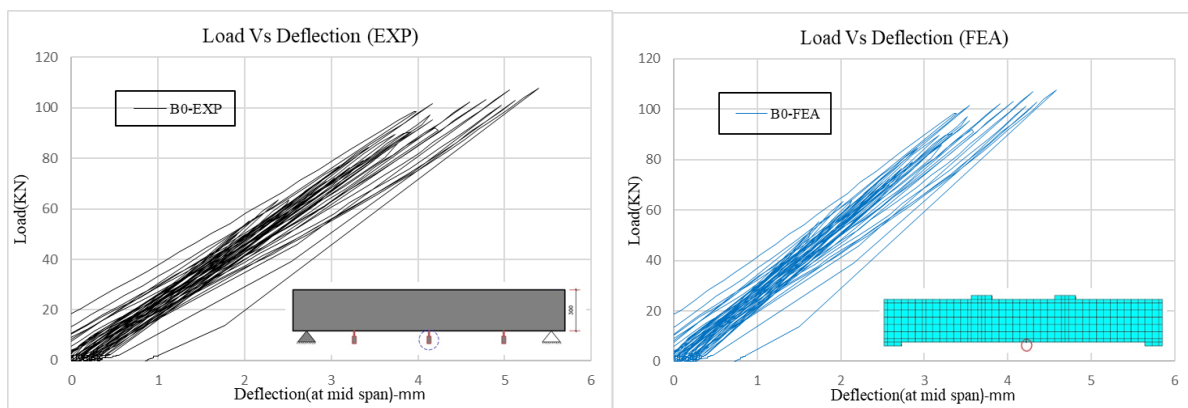


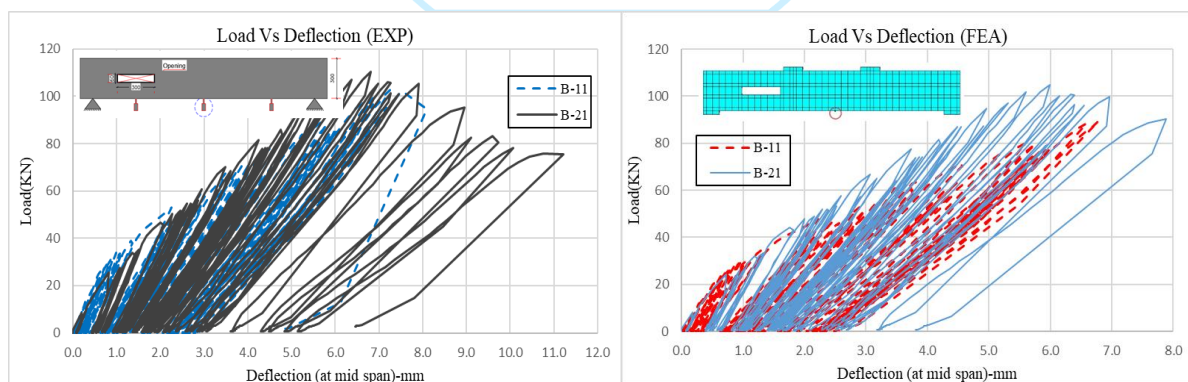
Fig.17 Deformation for tested specimens

4.3 Load Deflection Curves

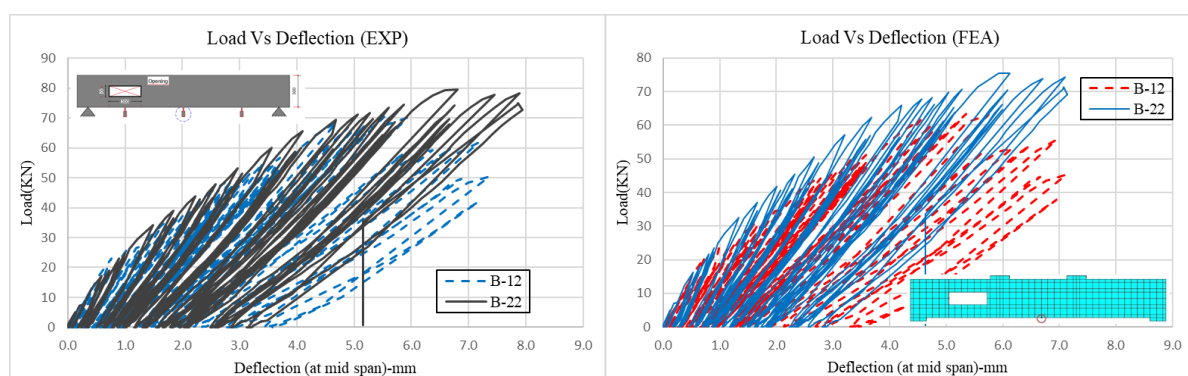
Through the analysis of beam deflection, it is apparent that the beams without diagonal reinforcement surrounding the openings showed a lower failure load compared to the beams with diagonal reinforcement surrounding the openings. Moreover, the failure load decreases as the height of the opening increases. In the case of a control beam (without openings), the failure occurred due to flexural stress. However, in beams with openings, the failure mode shifted to the shear zone as the height of the opening varied. The failure load of beams B11, B12, and B13 (i.e. without diagonal reinforcement around the opening) is observed to be decreased by 6%, 12%, and 14%, respectively, in comparison to the failure load of the beams B21, B22, and B23 (i.e. with diagonal reinforcement surrounding the opening). Figures 18 a, b, c and d show the deflection curves at the mid-span for specimens B0 (i.e. control beam), B11, B12, and B13 (i.e. without diagonal reinforcement around the opening) and specimens B21, B22, and B23 (i.e. with diagonal reinforcement around the opening) which are subjected to cyclic load. The average deflection values obtained from both experimental and finite element analysis for all beams in the mid-span are 7.65, 6.95, 6.10, 9.50, 7.55, and 5.40 mm, respectively. Similarly, Figures 19 a, b, c and d show the deflection curves at the opening for specimens B11, B12, and B13 (i.e. without diagonal reinforcement surrounding the opening) and specimens B21, B22, and B23 (i.e. with diagonal reinforcement surrounding the opening) which are subjected to cyclic load. The average deflection values obtained from both experimental and finite element analysis for all beams in the mid-span are 7.65, 6.45, 6.05, 8.00, 7.10, and 4.75 mm, respectively. Additionally, Figures 20 a, b, c and d show the deflection curves at the opposite to the opening for specimens B11, B12, and B13 (i.e. without diagonal reinforcement surrounding the opening) and specimens B21, B22, and B23 (i.e. with diagonal reinforcement surrounding the opening) which are subjected to cyclic load. The average deflection values obtained from both experimental and finite element analysis for all beams in the mid-span are 5.70, 5.55, 4.40, 6.25, 5.45, and 3.50 mm, respectively.



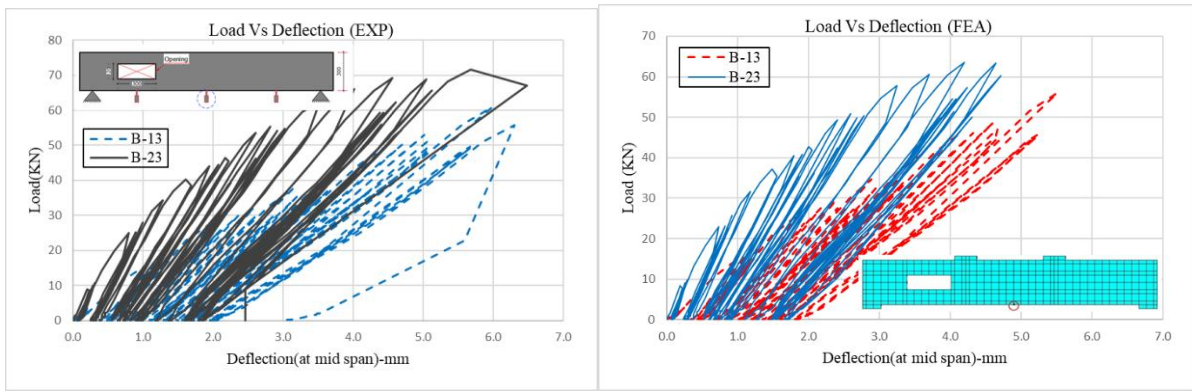
(a)



(b)

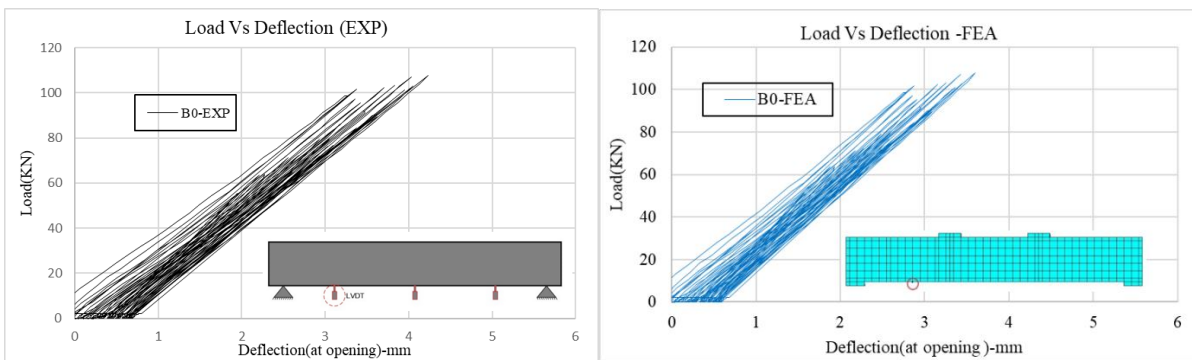


(c)

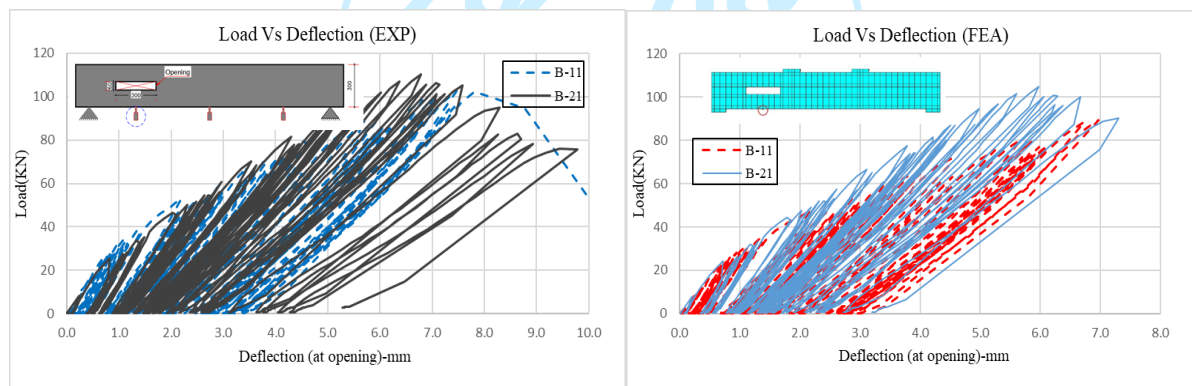


(d)

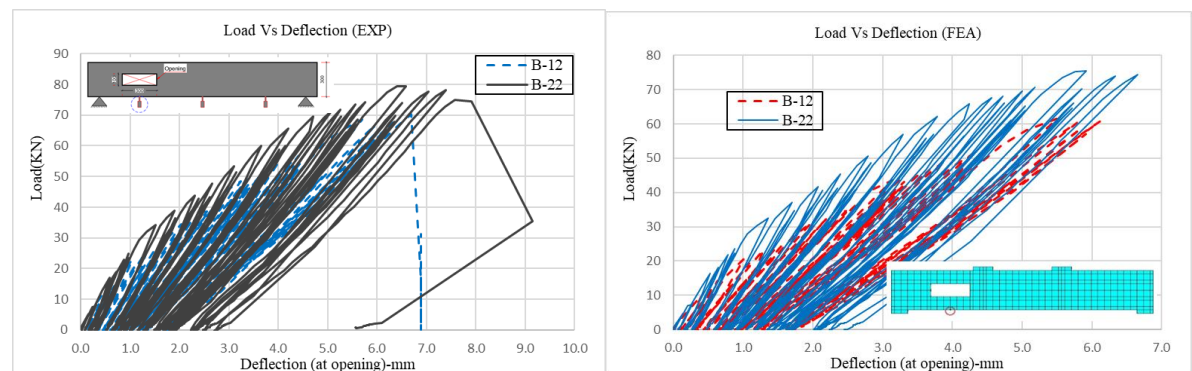
Fig. 18 Load versus deflection at mid span



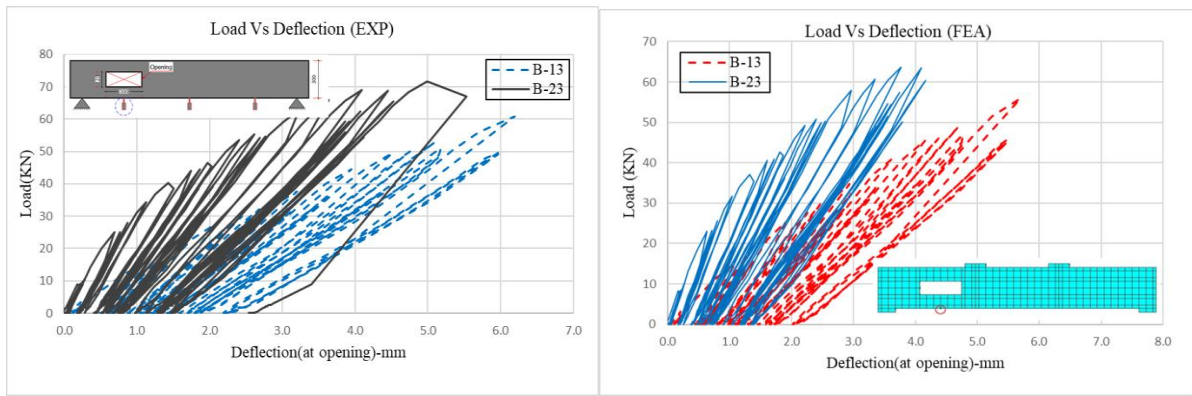
(a)



(b)

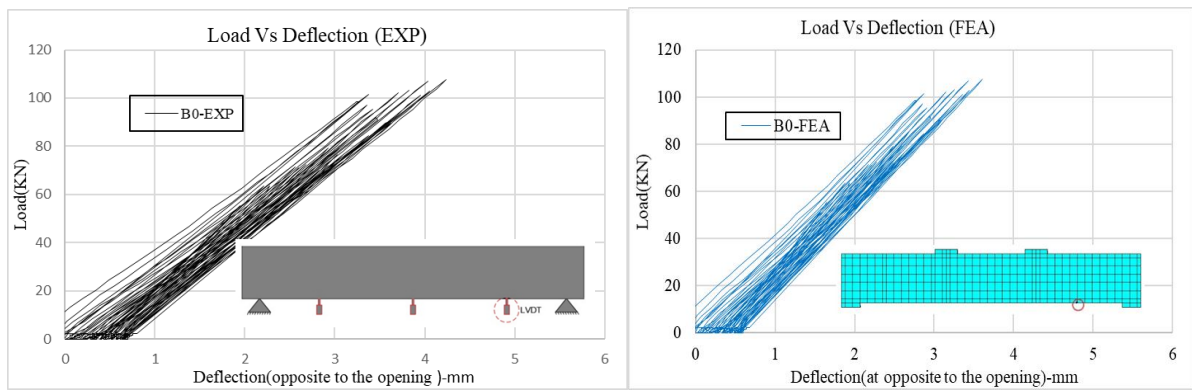


(c)

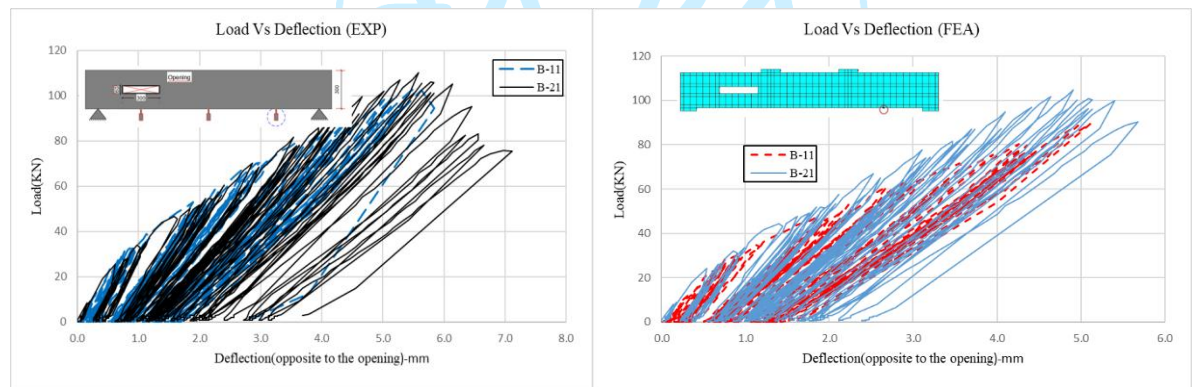


(d)

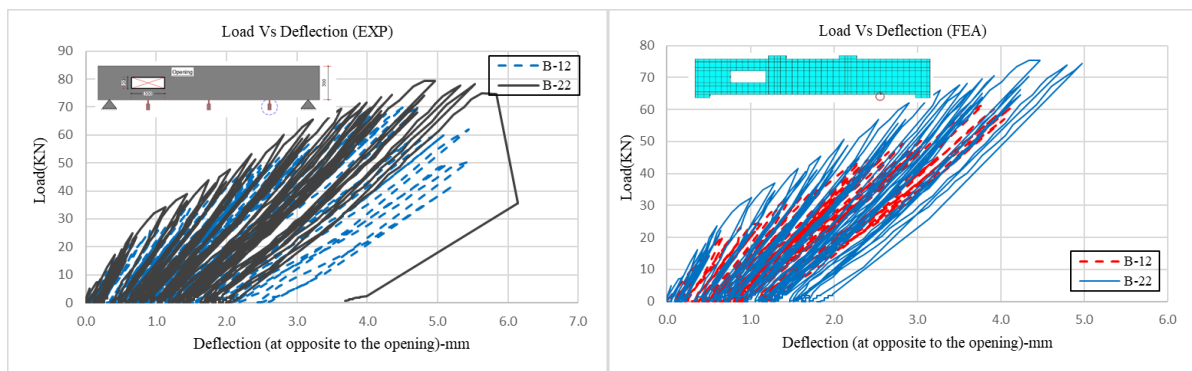
Fig. 19 Load versus deflection at opening



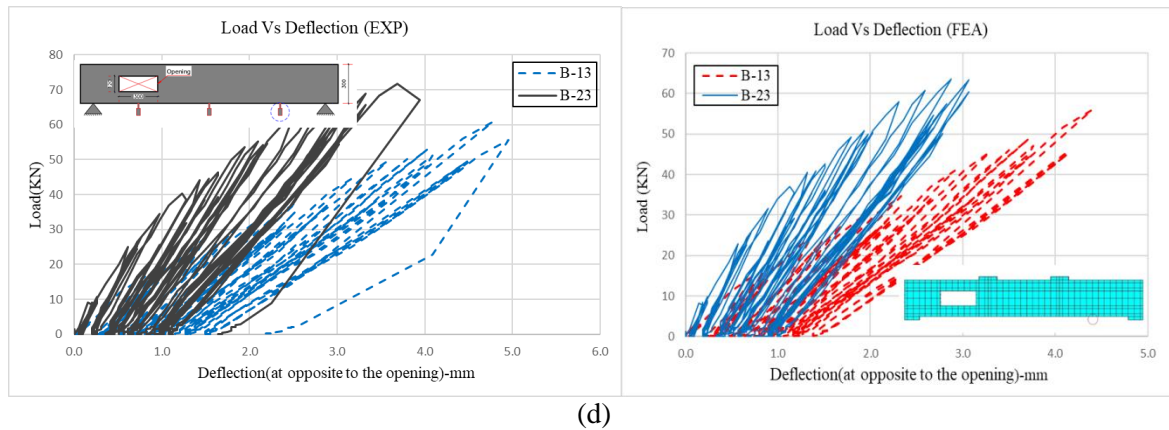
(a)



(b)



(c)



(d)
Fig. 20 Load versus deflection at opposite to the opening

5. Conclusions

This study examines the behavior of reinforced concrete beams with openings subjected to cyclic loads. The existence of openings in beams reduces the efficiency of the beam, hence decreasing the ultimate load capacity. The experimental results indicated that the failure load of a control beam under cyclic loads was 110 KN, while the failure load of a finite element analysis beam was 115 KN (i.e., 104%). The results were as follows: When we considered beams with openings and without diagonal reinforcement surrounding the opening, we found that the failure load decreased to 100 KN (i.e., decreased by 10% in the experiment) and 105 KN (i.e., decreased by 9% in the finite element analysis), respectively. A beam's failure load decreased to 68 KN when its opening was 30% of its height (i.e., decreased by 39%, experimental) and 72 KN (i.e., decreased by 38%, finite element). We determined the failure load for a beam with an opening of 40% of the beam height to be 60 KN (i.e., decreased by 45%, experimental) and 63 KN (i.e., decreased by 45%, finite element), compared to the control beam. On the other hand, the results showed, the beams with openings and with diagonal reinforcement surrounding the opening, when a beam with an opening equivalent to 20% of beam height was considered, the failure load decreased to 110 KN (i.e., decreased by 0%, experimental) and 108 KN (i.e., decreased by 6%, finite element). Likewise, A beam's failure load decreased to 80 KN when its opening is 30% of its height (i.e., decreased by 28%, experimental) and 77 KN (i.e., decreased by 33%, finite element). The failure load for a beam with an opening that is 40% of the beam height was determined to be 70 KN (i.e., decreased by 37%, experimental) and 70 KN (i.e., decreased by 40%, finite element), compared to the control beam. The results show that there is only a 10% difference between the failure loads found using experimental and finite element analysis. The results showed that beams without openings collapsed in the flexural region, whereas beams with openings collapsed in the shear zone. Cracks in beams without openings disperse throughout the entire beam. In contrast, the beams with openings and without diagonal reinforcement around the opening experienced cracks around the openings. In the case of beams with openings and equipped with diagonal reinforcement around the opening, the cracks did not concentrate around the opening only but rather spread at the support and in the mid-span, where their concentration increased as the height of the opening increased. For beams without openings, the deformation distributes uniformly in the middle area. The deformation shifts towards the opening and increases with the increasing height of the opening. The results indicate that the inclusion of inclined diagonal reinforcement around the opening enhances the performance of concrete beams by 15%.

References

- Huang, H., Li, M., Yuan, Y., & Bai, H. (2022). Theoretical analysis on the lateral drift of precast concrete frame with replaceable artificial controllable plastic hinges. *Journal of Building Engineering*, 62. <https://doi.org/10.1016/j.jobe.2022.105386>.
- Ghasemi, M., Zhang, C., Khorshidi, H., Zhu, L., & Hsiao, P. C. (2023). Seismic upgrading of existing RC frames with displacement-restraint cable bracing. *Engineering Structures*, 282. <https://doi.org/10.1016/j.engstruct.2023.115764>.
- Zhang, Z.; Li, W.; Yang, J. Analysis of stochastic process to model safety risk in construction industry. *J. Civ. Eng. Manag.* 2021, 27, 87–99. <https://doi.org/10.3846/jcem.2021.14108>.
- Huang, Y.; Zhang, W.; Liu, X. Assessment of diagonal macrocrack-induced debonding mechanisms in FRP-strengthened RC beams. *J. Compos. Constr.* 2022, 26, 04022056. [https://doi.org/10.1061/\(ASCE\)CC.1943-5614.0001255](https://doi.org/10.1061/(ASCE)CC.1943-5614.0001255).
- Özkılıç, Y. O., Karalar, M., Aksoylu, C., Beskopylny, A. N., Stel'makh, S. A., Shcherban, E. M., Qaidi, S., Pereira, I. da S. A., Monteiro, S. N., & Azevedo, A. R. G. (2023). Shear performance of reinforced expansive concrete beams utilizing aluminium waste. *Journal of Materials Research and Technology*, 24, 5433–5448. <https://doi.org/10.1016/j.jmrt.2023.04.120>.
- Wang, M., Yang, X., & Wang, W. (2022). Establishing a 3D aggregates database from X-ray CT scans of bulk concrete. *Construction and Building Materials*, 315. <https://doi.org/10.1016/j.conbuildmat.2021.125740>.

7. Shi, T., Liu, Y., Zhao, X., Wang, J., Zhao, Z., Corr, D. J., & Shah, S. P. (2022). Study on mechanical properties of the interfacial transition zone in carbon nanofiber-reinforced cement mortar based on the PeakForce tapping mode of atomic force microscope. *Journal of Building Engineering*, 61. <https://doi.org/10.1016/j.jobbe.2022.105248>.
8. Shi, T., Liu, Y., Hu, Z., Cen, M., Zeng, C., Xu, J., & Zhao, Z. (2022). Deformation Performance and Fracture Toughness of Carbon Nanofiber-Modified Cement-Based Materials. *ACI Materials Journal*, 119(5), 119–128. <https://doi.org/10.14359/51735976>.
9. Zhou, S., Lu, C., Zhu, X., & Li, F. (2021). Preparation and Characterization of High-Strength Geopolymer Based on BH-1 Lunar Soil Simulant with Low Alkali Content. *Engineering*, 7(11), 1631–1645. <https://doi.org/10.1016/j.eng.2020.10.016>.
10. Fang, B., Hu, Z., Shi, T., Liu, Y., Wang, X., Yang, D., Zhu, K., Zhao, X., & Zhao, Z. (2023). Research progress on the properties and applications of magnesium phosphate cement. In *Ceramics International* (Vol. 49, Issue 3, pp. 4001–4016). Elsevier Ltd. <https://doi.org/10.1016/j.ceramint.2022.11.078>.
11. Özkılıç, Y. O., Aksoylu, C., yazman, Ş., Gemi, L., & Arslan, M. H. (2022). Behavior of CFRP-strengthened RC beams with circular web openings in shear zones: Numerical study. *Structures*, 41, 1369–1389. <https://doi.org/10.1016/j.istruc.2022.05.061>.
12. American Concrete Institute, “Building Code Requirements for Reinforced Concrete”, Detroit, ACI-381M-11, (2011).
13. Egyptian Code for The Design and Construction of Reinforced Concrete structure, Cairo, 2020, Ministry of Housing and Development of New Communities, Cairo, Egypt.
14. Nmai, C. K., & Darwin, D. (1984). CYCLIC BEHAVIOR OF LIGHTLY REINFORCED CONCRETE BEAMS.
15. Amiri, J. V., & Hosseinalibygie, M. (n.d.). EFFECT OF SMALL CIRCULAR OPENING ON THE SHEAR AND FLEXURAL BEHAVIOR AND ULTIMATE STRENGTH OF REINFORCED CONCRETE BEAMS USING NORMAL AND HIGH STRENGTH CONCRETE. 13th World Conference on Earthquake Engineering, Vancouver, B.C., Canada, August 1-6, 2004, Paper No.3239.
16. Masoudnia, R. (n.d.). Investigation of the Oppening Effects on the Behavior of Concrete Beams without Additional Reinforcement in Opening Region Using Fem Method. <https://doi.org/10.13140/RG.2.1.2108.1041>.
17. Kumar, N. (2017). Behavior of Reinforced Concrete Beam with Opening. In *International Journal of Civil Engineering and Technology* (Vol. 8, Issue 7). <http://iaeme.com/Home/journal/IJCIET581editor@iaeme.comhttp://http://iaeme.comhttp://iaeme.com/Home/issue/IJCIET?Volume=8&Issue=7http://iaeme.com/Home/journal/IJCIET582>.
18. Kamonna, H. H., Alkhateeb, L. R., Kamonna, H. H., & Alkhateeb, L. R. (2020). STRENGTHENING OF REINFORCED CONCRETE DEEP BEAMS WITH OPENINGS BY NEAR SURFACE MOUNTED STEEL BAR. In *Journal of Engineering Science and Technology* (Vol. 15, Issue 4).
19. Bai, Y.-L., Dai, J.-G., & Teng, J. G. (2014). Cyclic Compressive Behavior of Concrete Confined with Large Rupture Strain FRP Composites. *Journal of Composites for Construction*, 18(1). [https://doi.org/10.1061/\(asce\)cc.1943-5614.0000386](https://doi.org/10.1061/(asce)cc.1943-5614.0000386).
20. [20] Li, B., Xu, L., Chi, Y., Huang, B., & Li, C. (2017). Experimental investigation on the stress-strain behavior of steel fiber reinforced concrete subjected to uniaxial cyclic compression. *Construction and Building Materials*, 140, 109–118. <https://doi.org/10.1016/j.conbuildmat.2017.02.094>.
21. Medic, S., Zivalj, E., Biberkic, F., Zlatar, M., & Hrasnica, M. (n.d.). EXPERIMENTAL STUDY ON BEHAVIOR OF REINFORCED CONCRETE BEAM SUBJECTED TO CYCLIC LOADING, 16TH EUROPEAN CONFERENCE ON EARTHQUAKE ENGINEERING, 18-21 JUN 2018.
22. Gião, R., Lúcio, V., & Chastre, C. (2019). Gravity load effects on the behaviour of reinforced concrete beam critical zones subjected to cyclic loads. *Engineering Structures*, 181, 503–518. <https://doi.org/10.1016/j.engstruct.2018.12.045>.
23. [23] Liu, T. J., Chen, S. W., Feng, Z. H., & Liu, H. Y. (2020). Effect of Web Openings on Flexural Behaviour of Underground Metro Station RC Beams under Static and Cyclic Loading. *Advances in Civil Engineering*, 2020. <https://doi.org/10.1155/2020/1210485>.
24. [24] Ribeiro, P. de O., Gidrão, G. de M. S., Vareda, L. V., Carrazedo, R., & Malite, M. (2020). Numerical and experimental study of concrete i-beam subjected to bending test with cyclic load. *Latin American Journal of Solids and Structures*, 17(3). <https://doi.org/10.1590/1679-78255880>.
25. Chiu, C. K., Sung, H. F., Chou, J. C., & Choudhury, S. R. (2024). Reinforcement methods of a reinforced concrete beam with the circular opening in the plastic hinge region under cyclic loading. *Advances in Structural Engineering*. <https://doi.org/10.1177/13694332241252273>.
26. Ahmed, A., Fayyadh, M. M., Naganathan, S., & Nasharuddin, K. (2012). Reinforced concrete beams with web openings: A state of the art review. *Materials and Design*, 40, 90–102. <https://doi.org/10.1016/j.matdes.2012.03.001>.

27. Salih, R., Zhou, F., Abbas, N., & Mastoi, A. K. (2020). Experimental investigation of reinforced concrete beam with openings strengthened using frp sheets under cyclic load. *Materials*, 13(14). <https://doi.org/10.3390/ma13143127>.
28. Agag, F., Salem, E., Ahmad & Sallam, H. (2022). Experimental assessment of different strengthening technique for opening of reinforced concrete beams, *Frattura Ed Integrità Strutturale* 59 (2022) 549-565; <https://doi.10.3221/IGF.ESIS.59.36>.
29. Elansary, A. A., Abdel Aty, A. A., Abdalla, H. A., & Zawam, M. (2022). Shear behavior of reinforced concrete beams with web opening near supports. *Structures*, 37, 1033–1041. <https://doi.org/10.1016/j.istruc.2022.01.040>.
30. Magdy Khalaf., Aboul-Nour, L., Khater, M. (2023). “Numerical nonlinear analysis of RC beams with un-strengthened and CFRP- strengthened opening drilled under service loads within shear zone” *Frattura ed Inteqrita Strutturale*, 63 (2023) 206-233; <https://doi.org/103221/IGF-ESIS.63.17>.
31. Lam, T. Q. K., Do, T. M. D., Ngo, V. T., Nguyen, T. T. N., & Pham, D. Q. (2020). Concrete grade change in the layers of three-layer steel fibre reinforced concrete beams. *Journal of Achievements in Materials and Manufacturing Engineering*, 102(1), 16–29. <https://doi.org/10.5604/01.3001.0014.6325>.
32. “ANSYS FEM.” [Online]. Available: WWW.ANSYS.com.
33. Hawileh, R. A., Rahman, A., & Tabatabai, H. (2010). Nonlinear finite element analysis and modeling of a precast hybrid beam-column connection subjected to cyclic loads. *Applied Mathematical Modelling*, 34(9), 2562–2583. <https://doi.org/10.1016/j.apm.2009.11.020>.

